5

Glial Tumors: Quantification and Segmentation from MRI and MRS

Weibei Dou[1] and Jean-Marc Constans[2]
[1]*Tsinghua University,*
[2]*CHU de Caen*
[1]*China*
[2]*France*

1. Introduction

Brain tumor segmentation is an important technique in computer-assisted diagnosis. To improve brain tumor diagnosis, it is necessary to use biochemical information provided by magnetic resonance spectroscopy (MRS). Some of the challenges involved are determining how to combine multimodal signals such as proton MRS and morphological or structural images, then knowing how to use the combined information to make a decision. In this paper, we propose using a data fusion method to perform an automatic segmentation of the brain tumor areas.

To diagnose brain tissue abnormalities such as tumors, we need to use multispectral magnetic resonance images (MRIs), e.g. T1-weighted, T2-weighted, gadolinium, or FLAIR to determine some properties of the tumor, including size, position, sort, and relationship with other tissues. However, the tumor type and grade are usually diagnosed from histopathological examination of a surgical specimen. Proton (^{1}H) magnetic resonance spectroscopy (MRS) is a non invasive MR technique that provides biochemical information about metabolites. The major biochemical characteristics can provide useful information about brain tumor type and grade (Howe et al., 2003a; 2003b). In many studies, the use of in vivo ^{1}H-MRS has been described for determining tumor type and grade (Howe et al., 2003a; Howe et al., 2003b; Preul et al., 1996; Majós et al., 2009).

Since analysis of in vivo MRS measurements are dependent on acquisition techniques that could compromise the spatial resolution and accuracy of resulting metabolite values (Maudsley et al., 2009), metabolic changes associated with disease are frequently small and diffuse. Furthermore, using the chemical-shift imaging (CSI) technique, metabolite images, known as MR spectroscopic imaging (MRSI) images, can be created using multivoxel MRS information, but it is not as visually interpretable as in a structural MRI (Maudsley et al., 2009). So, for tumor tissue classification, it is important that MRSI be combined with MRI to make a more accurate estimation of variations in metabolites, support hypotheses of metabolite variation causes, and to yield sufficient information about the tissue.

For over a decade, scientists have been developing automated brain-tumor classification methods using MRS (Garcia-Gomez et al., 2009), but a more clear definition of brain tumor type and grade may be obtained by combining MRS or MRSI and MRI (Garcia-Gomez et al., 2009). A technique used to differentiate glioblastoma from metastatic lesions using MRI and

MRS data has been published (Luts et al., 2009). Wang et al. described a classification of brain tumors using feature selection and fuzzy connectedness (Wang et al., 2007). These features are extracted from MRI and MRS data.

There are 2 difficulties for combining MRSI data and MRI data. Firstly, these data are presented in different modalities, so they do not have the same spatial resolution. There is very low spatial resolution per voxel for MRSI, and high spatial resolution per pixel for MRI. Secondly, one MR image corresponds to the distribution of many tissues, or many tissue structures. But one MRS image is an image which corresponds to 1 metabolite or a ratio between several metabolites. So, the different metabolite values cause variation in MRS images, as in the mapping of metabolite distributions by MRSI presented in a previous study (Maudsley et al., 2009). One of the main questions for application is how to combine these MRS images and MR images to give a good automated tissue classification result. The key point of the combination is how to model the metabolite distribution from MRS, which is coherent with information from MR images.

For an automated description of a brain tumor type and grade, we propose a modelization method of glioma tissues by combining the information from MR images and mulitivoxel MRS data. It can create an MRS-weighted MR image automatically, which retains the high spatial resolution of an MR image and the grey levels corresponding to biochemical abnormalities of pathological processes in brain tissues. The combined data of MRS and T2-weighted images should be enhanced by an operation of exponential companding. It consists of 5 steps: multi-voxel MRS (or CSI) data processing, localization and volume of interest (VOI) extraction, data combination, exponential companding, and region growing as the last step of segmentation. Data from 2 glioma patients, provided by Tiantan hospital in China, have been used to evaluate our method. Two “ground truth”, tumors with edema and tumor only, used for result comparison are with manual labels made by neuroradiologists at Tiantan and Nanfang hospitals in China. The segmentation result represents MRS-weighted T2 structure image in the tumor region. As a performance assessment, we obtain 99% correct detection for tumor only and 98% for tumor with potential edema, and a false detection rate of 9% and 6% inside VOI, respectively. The proposed method is also a simple information fusion strategy.

2. Quantitative analysis of glial tumor metabolism

Conventional magnetic resonance imaging (MRI) provides information about tumor anatomy, its extent, and pathology; however, the specificity of diagnosis used to distinguish between benign and malignant disease and the grade severity is still not optimal. Furthermore, MRI does not provide information on the underlying biochemical processes associated with tumor progression and potential regression under therapies. Thus, the biochemical information from tissues may be useful for specific diagnosis, accurate prognosis and follow-up of therapeutic response when used as an adjunct to anatomical details obtained from MR images. This can be achieved through in vivo proton Magnetic Resonance Spectroscopy (MRS) that provides unique metabolic information, at the molecular level, of diagnostic and prognostic importance for tumor typing and grading (Galanaud et al., 2007). The tissues contain several biologically important metabolites (biochemicals) in addition to water and fat hydrogen atoms that could be followed by MRS. It also provides information on the alterations in metabolic pathways during disease processes by detection and quantification of metabolites and their temporal variation. MRS

is also a useful tool in the planning and evaluation of treatments and in predicting tumor progression and treatment response. It is known that tumor growth is not a simple regulated phenomenon. There are variations in metabolism and cell density, and in the presence of cystic and necrotic regions (particularly in heterogeneous malignant tumors and under therapies). Thus, the MR spectrum obtained from tumor tissue can be a mixture of different tissue types, including those of different grades, which complicates the spectral interpretation. Most MRS measurements are based on the use of proton (^{1}H) nuclei, due to its great sensitivity. The integration of ^{1}H MRS with clinical MRI investigation is relatively straightforward and easy to implement. Addition of in vivo ^{1}H MRS protocol increases the overall acquisition time by approximately 10 to 20 minutes but it drastically improves the diagnostic, prognostic accuracy and the follow-up of therapeutic response. This method has generated considerable interest in recent years and the added value of the vivo ^{1}H MRS is in the process of evaluation in clinical application. In particular it would allow quantification of metabolites from a well-defined region of interest (ROI) or volume element (voxel). Moreover, the heterogeneous nature of tumors could be understood and detected, which would be of great interest for biopsy guidance in time and space (with CSI) and planning, monitoring, and evaluation of treatments (Soffietti et al. 2010) such as surgery, radiotherapy, and chemotherapy (Hart et al. 2008). Therefore, the possibility of obtaining in vivo quantitative biochemical information has revolutionized the field of clinical neurooncology. In the present work on gliomas, metabolic information obtained in quantitative single voxel MRS measurements, associated with anatomic and perfusion data, allows us to establish an accurate prognosis based on a spectral and metabolic classification system and start to evaluate therapies. In addition, in longitudinal follow-up studies, multimodality (with perfusion and with Positon Emission Tomography (PET) especially in glioblastomas) allow us to study the relationship between MRS, MRI segmentation and perfusion, together with some biologic parameters (eg, proliferation, infiltration, glycolysis metabolism, necrosis) thus helping to characterize sensitive biomarkers and to detect early changes in order to assess costly and heavy (for the patient) therapies rapidly and more accurately. Moreover, MRS data to be evaluated have to be related to data such as the response to therapy, histology, and genetic prognostic mutations (Isocitrate Dehydrogenase 1 IDH1, 1p19q, Methyle guanine methyl transferase MGMT).

Numerous studies reported in the literature have shown that ^{1}H MRS contributes significantly to the management of brain tumors. The major metabolites seen at long, intermediate, and short echo times are N-Acetyl-aspartate (NAA; 2.02 ppm), total creatine (tCr; 3.03 ppm), and choline-containing compounds (tCho; 3.2 ppm). NAA is found predominantly in neurons. The tCr level is reduced in astrocytomas and is nearly absent in meningiomas and schwannomas, indicating changes in energy metabolism. Gliomatosis cerebri is an uncommon and infiltrative type of glioma which is difficult to diagnose but has higher levels of tCr, thus distinguishing it from low grade gliomas (Galanaud et al., 2003). The tCho/tCr ratio increases with the grade of the glioma (Gill et al., 1990) but the large overlap of ratios between grades prevents its individual use as a reliable grading index. The level of tCho increases from grade II to grade III in astrocytomas, but grade IV tumors show wide variation due to the heterogeneity in cell density and necrosis. It is even more variable in gliomatosis. The ratio tCho/NAA was shown to correlate with long-term survival independent of tumor type (Nelson et al., 2002). In addition to the above predominant metabolites observed at long echo times, additional metabolites such as Glx (glutamate

(Glu) and glutamine (Gln), at 3.6-3.9 ppm and 2.1- 2.6 ppm) and myo-inositol (mI, at 3.56 ppm) are seen at shorter echo times and these also have diagnostic and prognostic potential. Lactate (a doublet at 1.33 ppm) is observed in tumors resulting from glycolysis (Stubbs et al., 1995), and lipids (1.3 and 0.9 ppm) are seen in high grade tumors (Howe et al., 2003a; Auer et al.,2001; Kuesel et al., 1994).
For evaluating therapies, one of the purpose is to better understand glial tumor metabolism and post chemotherapy, radiotherapy, and antiangiogenic variations. To determine cerebral variation in MRS area, amplitude, and ratios of metabolites and spectral profiles during a 6-year longitudinal follow-up in 26 patients with low grade gliomas (oligodendroglial tumors (n=12) or gliomatosis (n=14)) without initial hyperperfusion and treated with Temodal and to detect differences in infiltration (NAA), proliferation (Cho/Cr), necrosis (lipids), glycolytic metabolism (lactate) or energetic metabolism (glucose and glutamine) at different tumoral stages and after therapies. Gliomatosis Cerebri (GC) is a challenging tumor, considered to have a poor prognosis and poor response to treatment.

2.1 Materials, methods and measures

2.1.1 Patient population

The World Health Organization (WHO) classification of gliomas is based on the presumed cell origin, and distinguishes between astrocytic, oligodendrocytic, and mixed gliomas. A grading system is based on the presence of the following criteria: increased cellular density, nuclear atypia, mitosis, vascular proliferation, and necrosis. The main histological subtype of grade I gliomas is pilocytic astrocytoma, which is benign. Diffuse astrocytomas, oligodendrogliomas, and oligoastrocytomas are low grade (II) or high grade (III and IV) tumors. Glioblastomas correspond to grade IV astrocytomas.
We studied glioblastomas and mainly low grade gliomas (oligodendrogliomas and gliomatosis).

2.1.2 MRI acquisition and segmentation

Measurements of Sagittal T1, axial proton density, T2, FLAIR, diffusion, perfusion, 3D T1 and 3D T1 planes after gadolinium were acquired (Fig. 1c). Total tumoral volume, volume of FLAIR and T2 hypersignal, contrast enhancement, hyperperfusion, and necrosis volumes are available on the MRI. A late enhancement should be taken into account. Segmentation allows a more quantitative multispectral MRI analysis to estimate tumor volumes, edema and necrosis (Fig. 1a and 1b, (Dou et al., 2007a; Dou et al., 2006; Constans, 2006)). These data allow us to show that treated tumor volumes, observed on MRI, change little between 2 measurements, while spectroscopic profiles and Cho/Cr or mI/Cr ratios decrease (see in Results of spectroscopy).

2.1.3 Perfusion

This NMR technique allows us to study cerebral microcirculation with very fast slice acquisition after gadolinium injection (first past perfusion). In glial tumor, the map of relative CBV ratio is proportional to area under the curves to evaluate tumoral vascularization after intravenous gadolinium injection and showing hyperperfusion.
The data show some tumoral angiogenesis with severe lesions of the BBB (blood-brain barrier). The extravasation of radiocontrast agents induces suceptibility changes, an increase in the curve area of first passing above the baseline. Only a few low grade gliomas

(gliomatosis and oligodendrogliomas) have shown hyperperfusion (without contrast enhancement) at the beginning. Then, more hyperperfusion and small amounts of contrast enhancement appear during the progression.
The relative Cerebral Blood Volume (rCBV) in low grade gliomas is not often elevated, between 1 and 3, showing relative hyperperfusion compared to the contralateral side.
This technique has high temporal resolution and low S/N, and relatively low spatial resolution. For this reason, there is interest in the fusion of perfusion data with MRI data (T1, gadolinium T1, FLAIR and T2).

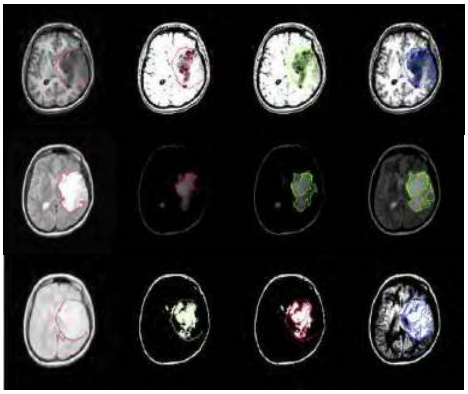

a) Manual segmentation and tissue classification of the different compartments from different weighted (T1, T2 and proton density) images from an oligodendroglioma that became gliomatosis

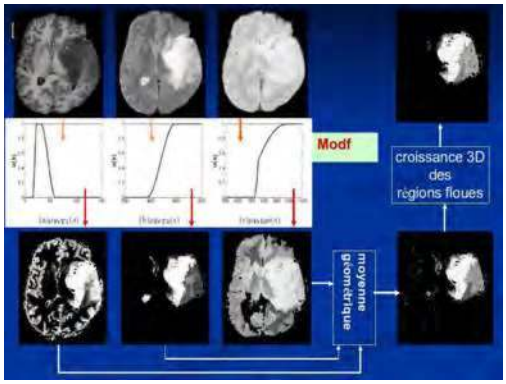

b) Segmentation, classification, and fusion of an oligodendroglioma that became gliomatosis

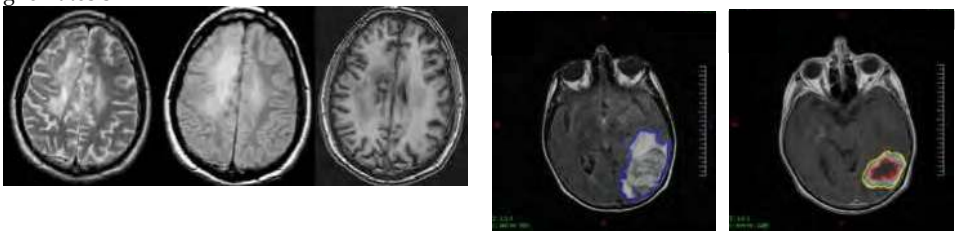

c) Gliomatosis and glioblastoma after segmentation

Fig. 1. MRI acquisition and segmentation of different types of gliomas,

2.1.4 MRS Acquisition and data processing

Single voxels (6 to 12 cm^3) from a 1,5 T machine were done on the most aggressive area (Fig. 2b and 2c) and in the contralateral side (Fig. 2a) using PRESS MRS sequence and with multiple TEs (35, 144, 288, 432ms).
MRS acquisition is sensitive to some parameters and some instrumental problems: localization quality, saturation bands, and homogeneity (Constans, 2006). This is even more evident in large volumes like CSI. SA/GE software (Fig. 3a) and a home-written SCI-MRS-LAB (Delcroix, 2000; Chechin, 2001) (Fig. 3b) (at CHU and Caen University and in Scilab INRIA-ENPC open source code) automated processing software packages yield amplitudes,

areas, ratios, and relative concentrations. Quantification based on amplitude and area (proportional to concentration and relaxation) estimation in spectral domain needs solvent resonance(s) suppression and presents some difficulties such as unknown resonances and molecule metabolization. This process requires normalization with a relative scale with a ratio to another metabolite such as water, NAA, Cr, or absolute metabolite concentration (absolute scale).

Data Processing

There are few quantification methods (SA/GE, JMRUI, SCI-MRS-LAB, THU-MRS0.5 (Dou et al., 2009), THU-MRS1.0 (Chi et al., 2011), sparse representation (Guo et al., 2010), which include different processing steps, e.g. water suppression, baseline estimation, fitting and analysis (Provencher et al., 1982; Nelson, 1989; Nelson, 2001; Hossu, 2009). Fig. 3 shows an example of a quantification methods comparison between Vendors such as SAGE (Spectroscopy Analysis by General Electric) (Fig. 3a) and SCI-MRS-LAB (Fig. 3b).

Usually, we can obtain much better water signal suppression and baseline estimation with SCI-MRS-LAB than with SAGE, especially for overlapped coupled spins, eg, glutamate and glutamine, citrate, or unusual additional resonance to fit.

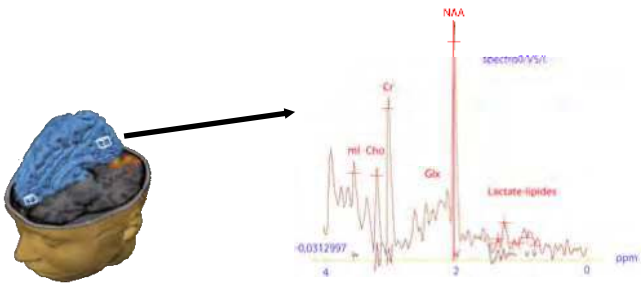

a) Magnetic resonance spectroscopy single voxel short TE 35 ms spectrum from white matter contralateral side similar to a normal spectrum

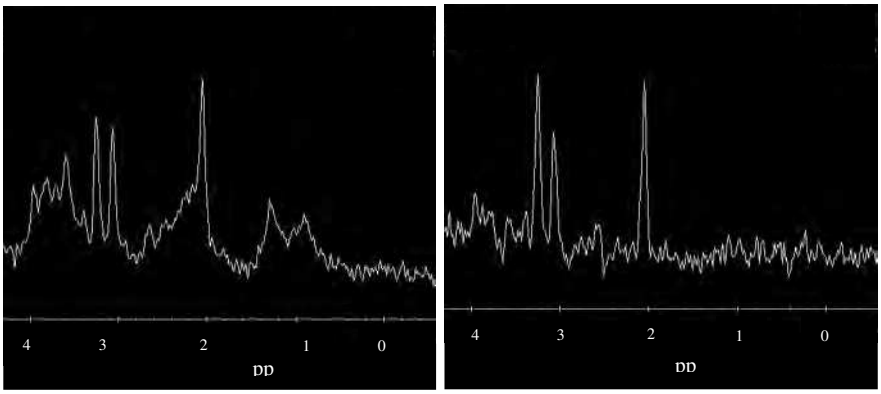

b) Example of spectra from gliomatosis tumor onset at 1.5 Tesla in PRESS sequences at different TE: 35 ms (left) and 144 ms (right) and showing infiltration (NAA/Cr decrease), gliotic activity (slight increase of mI and Cr) with some lactate and demyelination compared to onset ,

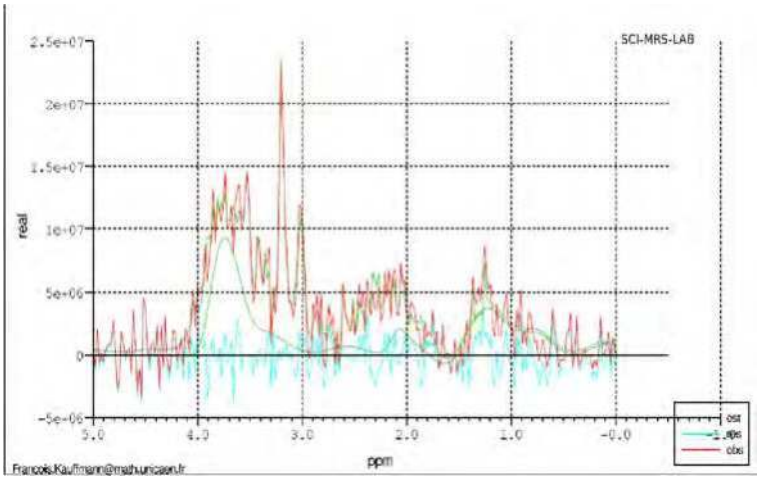

c) Example of spectral variations in glioma modelized by SCI-MRS-LAB processing software:

Cho (containing mainly the metabolites glycerophosphocholine (GPC) and elevated phosphocholine (PC) at 3.22 ppm): proliferation
Lactate (at 1.33 ppm): glycolysis
Decreased NAA/Cr (NAA at 2.02 ppm and Cr at 3.03 ppm): infiltration

The raw signal is in red, modelization by SCI-MRS-LAB, in green, baseline in green, and residuals in blue.In this example, Cho/Cr and mI/ Cr decrease under chemotherapy (Temozolomide [Temodal ®]). NAA/Cr ratios are variable and have a tendency to improve under Temozolomide in gliomatosis.

Fig. 2. MRS acquisition and modelization from a health volintier 2a), and giloma tumors 2b) and 2c)

After therapy, a study of the contralateral side is very important to assess effects of these therapies on the remaining non tumoral neuronal tissues.

Statistical Analysis

In segmentation, tissular classification, and FLAIR hypersignal extension volume the largest variation between n+1 and n exams was retained. Statistical analyses of longitudinal spectroscopic data with z_{test} were done (every 3 months over 60 months).
The longitudinal evolution of Cr concentration was calculated and, because of its low concentration variation in time, this metabolite was used as the reference for the different metabolite ratios. Then, Cho/Cr, NAA/Cr, Myoinositol/Creatine (mI/Cr) and Choline/N-Acetyl-Aspartate (Cho/NAA) were used; their longitudinal variations were studied and analysed.

2.2 Results

2.2.1 Segmentation

The segmentation of gliomas is easier to measure than the segmentation of gliomatosis, especially when assessing contrast enhancement, necrosis and total volumes. In these glioma cases, methods of mathematical morphology or classifications, e.g. Support vector machine (SVM) can be used. The segmentation of glioblastomas and oligodendrogliomas is also easier than gliomatosis because in this type of glioma with more infiltration, it is

difficult to separate the different tumoral compartments and to accurately judge the extent of the infiltration, especially when there is little edema and small contrast differences.

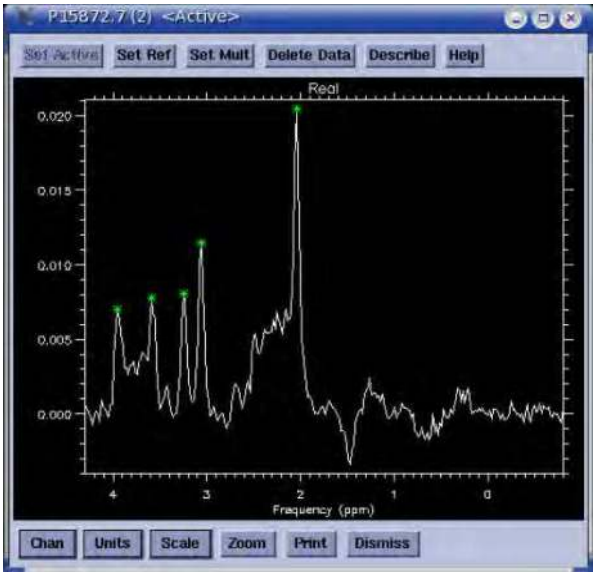

a) Spectral analysis software from General Electric (SA/GE)

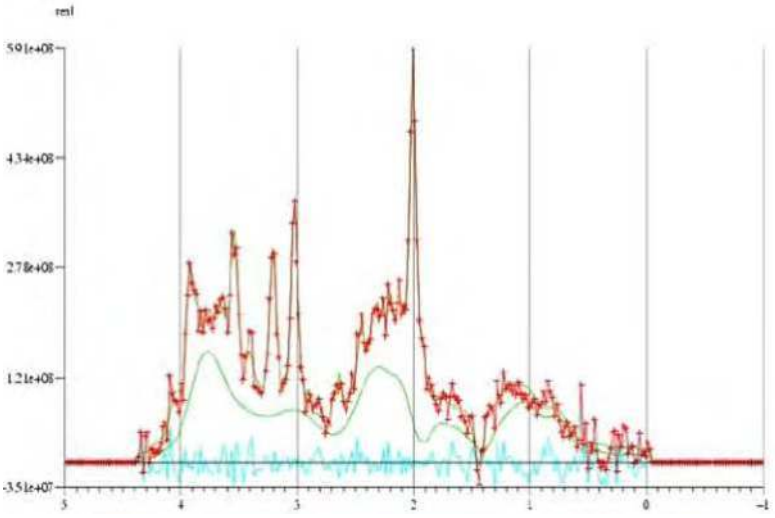

b) The raw signal (in red), modelization by SCI-MRS-LAB (in green the signal), base line (in green) and residuals (in blue)

Fig. 3. Example and comparison of SAGE (Figure 3a) and SCI-MRS-LAB (Figure 3b) processing for short TE spectra from a normal healthy volunteer, ,

2.2.2 Spectroscopy results

Treated (with chemotherapy or radiotherapy) tumoral volumes in MRI, change little (< 20 %) in low-grade gliomas between 2 exams, while spectroscopic profiles and ratios do change (> 60 %) with increases in NAA/Cr and decreases in cho/Cr or mI/Cr ratios, sometimes with a tendency to return to more normal values (even in some gliomatosis lesions).
Without chemotherapy, spectroscopic profiles worsen, with increases in Cho/NAA, Cho/Cr and mI/Cr ratios, decreases in NAA/Cr and sometimes with increases in lactate.
After chemotherapy, treated tumoral volumes in MRI change little between 2 exams, while spectroscopic profiles and ratios do change. MRS could, in fact, be more sensitive than MRI and could, in some cases, be predictive of worsening.

2.2.3 Results of longitudinal follow-up

Some patients with low grade gliomas are still alive 10 years after diagnosis, whereas for glioblastoma, we only obtained a few measures because the patients died within 2 years, on average. Therefore, we will present longitudinal follow-up studies of low grade gliomas (oligodendroglioma and gliomatosis) (Fig. 4).
Water and creatine are quite stable, which could justify using them for some other ratios to quickly detect spectroscopic variations. Cho concentration was predictive in 12 of 26 cases and more sensitive than ratios (8/26). Cho concentration increased in 5 patients with subsequent aggravation.

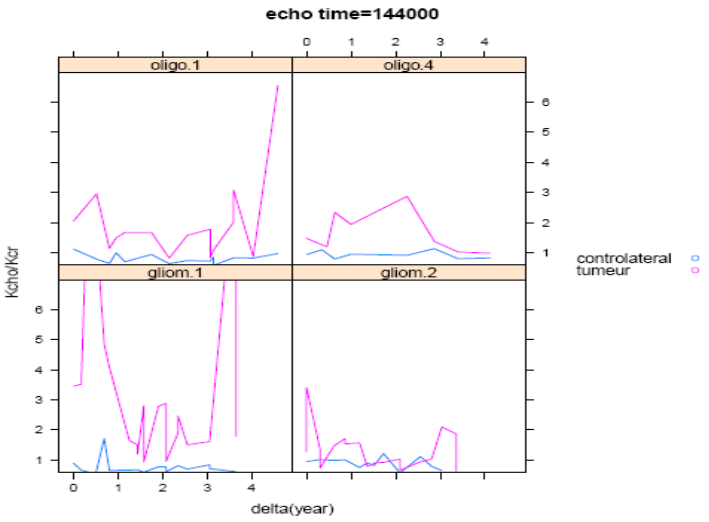

Fig. 4. Progression with time of a metabolite ratio under treatment: Cho/Cr in oligodendroglioma (above) and in gliomatosis (below).

Cho/Cr seems to decrease more rapidly and more frequently between exams in gliomatosis than in oligodendrogliomas. There is sometimes a decrease in the Cho/Cr ratio, but also an increase in the mI/Cr ratio (as in Fig 5).
Concentration of NAA has a tendency to increase with time under Temozolomide, more in contralateral, but sometimes in the tumor as well. NAA/Cr ratios are variable and seem to

improve with treatment in gliomatosis, but sometimes they show a decrease that precedes increased atrophy with FLAIR and T2. Effect of TE on measurements: concentration of NAA always shows a higher estimation on the short TE , while lactate shows a higher estimation on long TE.

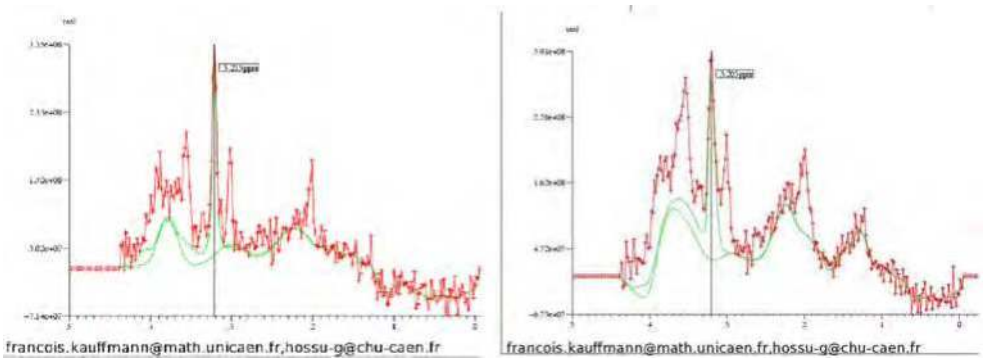

Fig. 5. Example of Cho/Cr ratio decrease under Temodal, but increase in mI/Cr ratio.

2.2.4 Example of perfusion and spectroscopy cases under antiangiogenic therapy

Later in the progression in 4 patients with hyperperfusion which disappeared with antiangiogenic therapy, but proliferation, infiltration, and glycolytic metabolism remained at a high level or worsened. (Fig. 6)

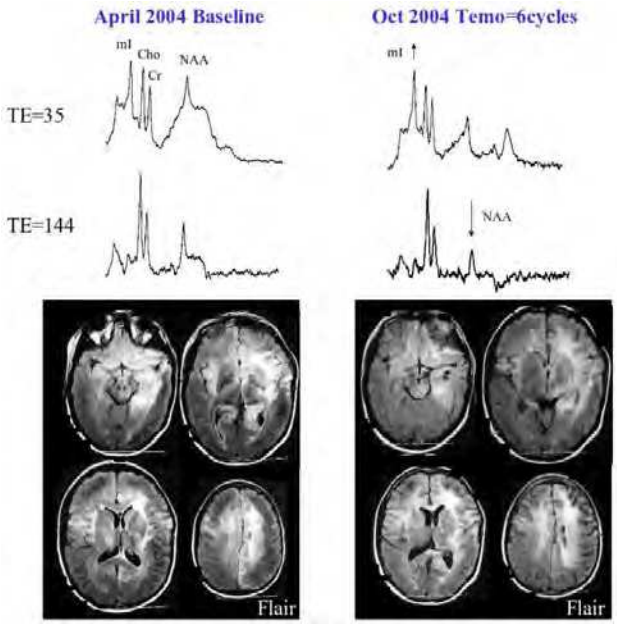

a) Example of MRI and MRS follow-up of a patient with gliomatosis

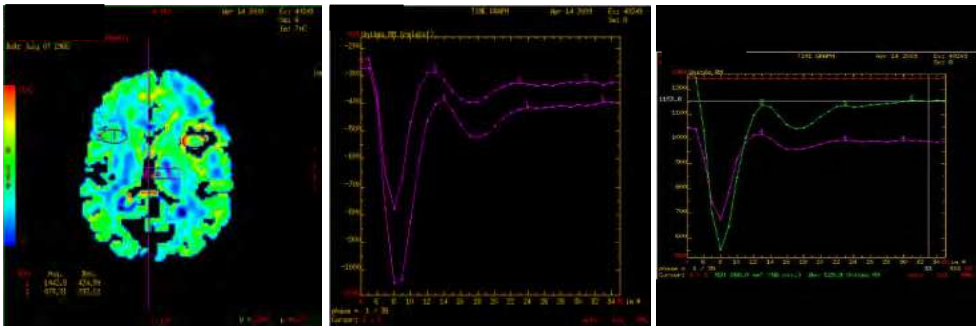

b) Example of MR Perfusion in another gliomatosis patient with decreased hyperperfusion that normalizes

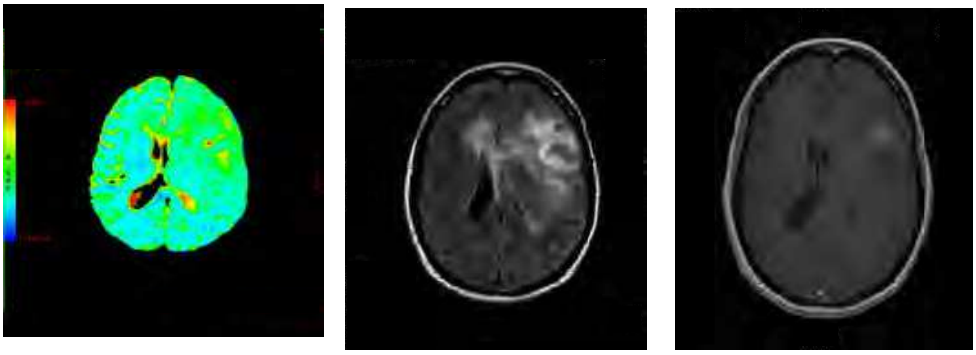

c) Diffusion, FLAIR, contrast enhancement: stability in diffusion and ADC, with FLAIR, and persistent contrast enhancement

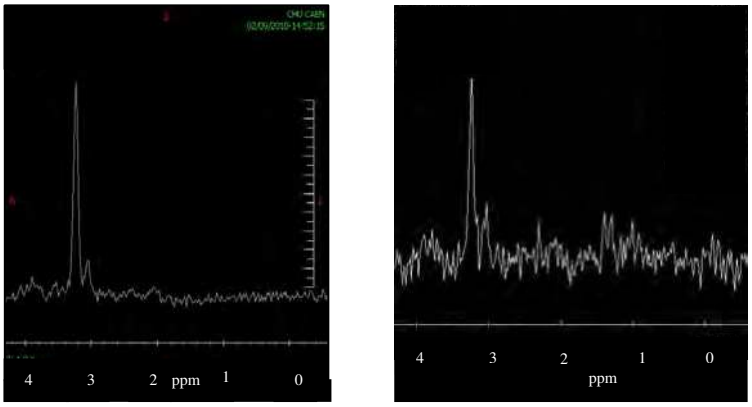

d) MRS: Increased proliferation (Cho at 3,22 ppm), glycolytic metabolism (lactate at 1,27-1,33 ppm), and infiltration (NAA at 2,02 ppm) at TE 144 and TE 288 ms

Fig. 6. Patient with good perfusion response to antiangiogenic treatment (Fig. 6b), but with a small amount of persistent contrast enhancement (Fig. 6c), intense increased proliferation, glycolytic metabolism, and infiltration (Fig. 6d)

3. Segmentation of brain tumor tissues using information fusion of MRI and MRS

For automated segmentation of brain tumor area, we have proposed a fuzzy information fusion based method (Dou, 2006; Dou et al., 2007a; Dou et al., 2007b), using T1-, T2-weighted and proton-density images. It is a feature fusion system, but it misses important biochemical information. The major biochemical characteristics can non invasively provide useful information on brain tumor type and grade (Howe et al., 2003b). Therefore, we propose a data-fusion strategy to segment brain tumors. This is an exponential companding method for enhancing the combination data from T2-weighted image and CSI signal. It automatically creates an MRS-weighted T2 structure image, which retains the high spatial resolution and brain structure information of the MR image while its grey levels correspond to the deterioration of brain tissues. The biochemical information is coherent for representing tumor grade and the deterioration of brain tissues. It is the key step in feature fusion for creating the feature models of glioma tissues, both for MRS values and for MR images. The combination modeling of these 2 types of information should separate the glioma tissues and normal tissues.

3.1 Features in models of glioma tissues

According to research done on brain tumor diagnosis by MR imaging and MRS, we can summarize 2 types of characteristics of glioma: one is the signal intensity of T1-weighted (with or without gadolinium) and T2-weighted images, and the other is the chemical-shift values of metabolites presented in MRS data.

3.1.1 Signal intensity characteristics of MR images

We have proposed some fuzzy modeling methods of different tumoral cerebral tissues on MR images based on fusion of tissue features (Dou et al. 2005a; 2005b; Dou, 2006; Dou et al., 2007a). Table 1 describes the characteristics of brain tissues by creating a gradation of signal intensity as a function of different tissues and MRI sequences (Dou et al., 2005a), where CSF is cerebral spinal fluid, GM is gray matter, and WM is white matter. In Table 1, the "Seqs" is used for "Sequences of MRI". The symbol "+" represents a hyper-signal; it means that the signal intensity is very high and the image is very bright. The symbol "-" represents a hypo-signal; the intensity is very low and the image is very dark. The symbol "-+" means that the signal intensity is higher than hypo-signal, and "+-" means that it is darker than hyper-signal. "- -" means that the signal intensity is lower than the hypo-signal, and "++" means that it is brighter than the hyper-signal.
Examples of T1-weighted image noted as T1, and T2-weighted image noted as T2 are shown in Fig. 7.

Sequences	**Graduality of signal intensity**					
	CSF	*GM*	*WM*	*Glioma*	*Edema*	*Necrosis*
T1	----	-	+++	---	--+	----
T2	+++ +	+	--	++	+++	++-

Table 1. Signal intensity characteristics of brain tissues on MR images.

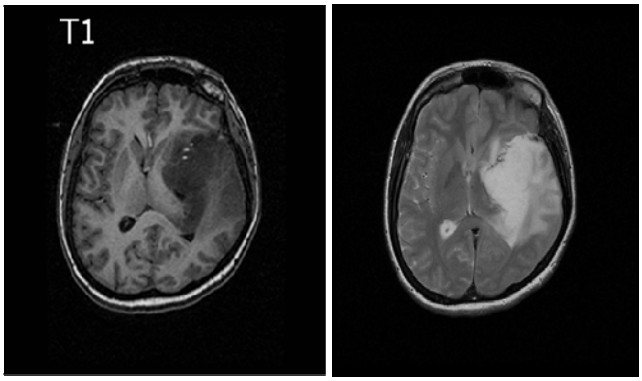

a) b)

Fig. 7. Original MRI images (a) T1 image, (b) T2 image

3.1.2 Features of metabolite changes in MRS

Among the large number of metabolites in the human body, there are only some that correspond to glioma. These include N-acetyl-asparate (NAA), creatine (Cr), choline (Cho), myo-inositol (mI), lactate (Lac), and free lipids (Lip). The variation in these metabolites can be ordered in a scalar form, as shown in Table 2, where the scalar order is: absent, very low, low, moderately (mod.) low, medium, moderately (mod.) high, high, or very high, which correspond to metabolite values from 0 to maximum. The metabolic changes with brain tissues are shown in Table 3. Data was obtained from previous studies (Brandao et al., 2003; Constans, 2006; Hoa, 2009; Dou et al., 2009).

Metabolite level	absent	very low	mod. low	low	medium	mod. high	high	very high
abbreviation	A	VL	LL	L	M	LH	H	VH

Table 2. Scalar description of metabolite values

Metabolite	**variation of metabolites corresponding with brain tissues**					
	CSF	***GM***	***WM***	***Glioma***	***Edema***	***Necrosis***
NAA	VL	VH	H	L/VL	M	A
Cho	A	M	LH	H/VH	LH	A
Cr	L	H	H	M/L	LL	A
mI	L	M	LH	H	LH/M	A
Lip	A	VL	L	H	L	VH
Lac	LH	VL	A	VH/H/LH	LH	H

Table 3. Metabolite change features in brain tissues on MRS

The metabolite-ratio characteristics of brain tissues, noted as *MetaR* and shown in Table 4, representing the *MetaR* characteristics of glioma, edema, and necrosis, are enhanced and the normal tissues are reduced. They correspond to signal intensity characteristics of the T2-weighted image described in Table 1.

Metabolite	variation of metabolites corresponding with brain tissues					
	CSF	*GM*	*WM*	*Glioma*	*Edema*	*Necrosis*
Cho/NAA	A	VL	L	VH	H	A
Cho/Cr	A	L	L	H	H	A
mI/Cr	M	L	M	H	H	A
Lip/Cr	A	VL	VL	H	M	VH
Lac/Cr	LH	VL	A	H	H	H

Table 4. Metabolite ratio characteristics of brain tissues

3.2 Data combination

There are 2 steps in the stage of data combination. The first, an important operation, is data localization, similar to data registration, used to adjust different data into a common coordination space. The second step is the actual combination.

3.2.1 Data localization

The operation of data localization is used to locate the MRS data to the CSI data, similar to a registration process. As their position vectors, recorded in the header of raw data, are under the same space coordinate, the volume of interest (VOI) field of MRS could be aligned to the image with the help of voxel spacings and position vectors. As shown in Fig. 8, the green grid represents the planar position of the voxels of a CSI on its reference image.

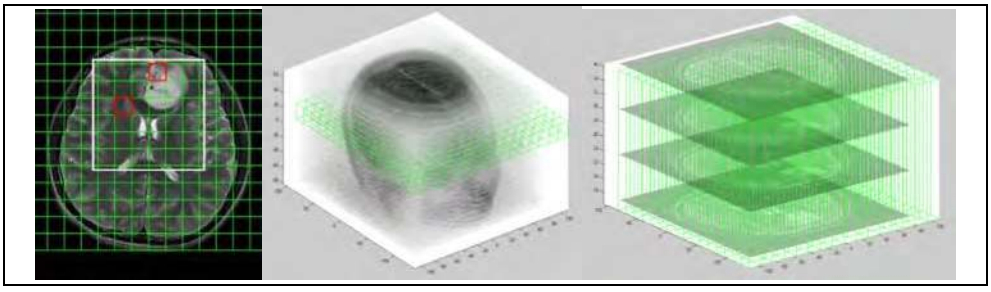

Fig. 8. An example of data location of MRS and T2 (left), the localization results are shown in 3D coordinate space (middle and right)

3.2.2 Data combination

Data combination is done as a multiplication operation as in (1). The MRS ratio is noted as *MetaR*(*i*,*v*), where "*i*" is the metabolite index and "*v*" is the voxel index of CSI. The MR image is noted as *MRIm*(*p*, *g*), where "*p*" is the pixel index, and "*g*" is the grey level of the MR image. Normally, *MetaR* is a function of the voxel determined by the CSI slice shown in Fig. 9. So, it is a 2-dimensional function noted as *MetaR*(*i*,*v*). For the same reason, *ComIm* can be created as a 3-dimensional function, noted as *ComIm*(*v*, *p*, *g*), where "*p*" is the pixel index corresponding to *MRIm*, and "*g*" is the grey level of a selected MR image and corresponds to "*p*". In fact, *MRIm* is a 2- dimensional function noted as *MRIm*(*p*, *g*), where

$$g \in \mathbf{G}, \text{ and } \mathbf{G} = \{T1, T2, PD, FLAIR, Gado, Diffusion, Perfusion...\}$$

Consider 2 variables: *MRIm* and *ComIm*. *MRIm* is a given image like T2 and *ComIm* is an estimated image. The correlation model *MetaR* can be considered as some relationship between them. So, the regression-like model for estimating GlioIm from *MRIm* can be created as in equation (1).

$$ComIm(v, p, g) = MetaR(i, v) \Theta MRIm(p, g) \tag{1}$$

where "Θ" denotes a necessary operator and "*p*" corresponds to "*v*". If a linear regression is necessary, equation (1) can be rewritten as (2):

$$Glio\,\mathrm{Im}(v, p, g) = MetaR(i, v) \times MR\,\mathrm{Im}(p, g) + MetaR(j, v) \tag{2}$$

where "*i*" and "*j*" indicate different metabolites.

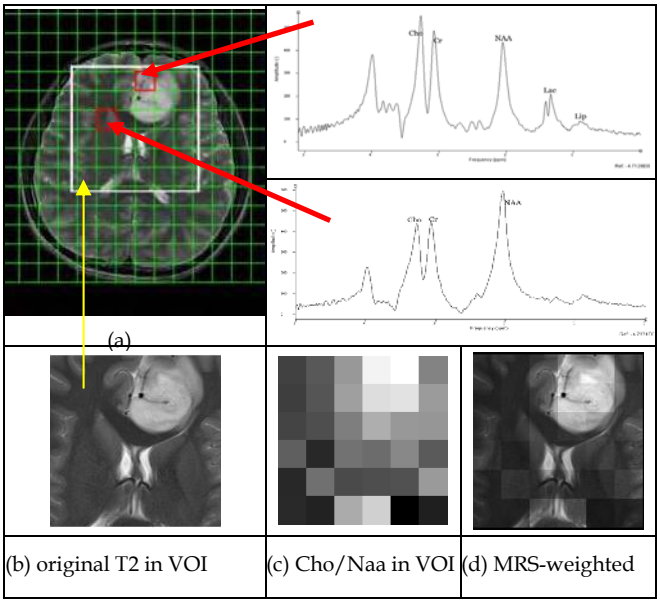

(b) original T2 in VOI (c) Cho/Naa in VOI (d) MRS-weighted

Fig. 9. Example of data combination of MRS and T2-weighted image. (a) is location image of CSI with VOI label (white line) on T2. The original image inside the region of VOI is enlarged and shown at (b). Two processed MRS resulting from step 1 are shown in the top right, corresponding to the voxels of CSI at the position of (1,4) and (3,2) of VOI, respectively. MRS ratio in (c) and combined image in (d).

T2 with localization information of CSI data is shown in Fig. 9 (a). Because MRS is available inside a VOI, marked with 6×6 white squares in Fig. 9(a), the combination of T2 and MRS should be done inside the VOI. Since the VOI contains multiple image slices, 1 MRS voxel corresponds to multi-pixel and multi-slices of an image.
Two examples of MRS are shown in Fig. 9 on the upper right. The top figure is MRS of a tumor voxel with coordinates (1, 4) in the VOI, and the bottom figure is that of normal tissue located

in (3,2) of the VOI. The ratio of Cho/Naa for each voxel is shown in Fig.9(c). The data combination of MRS and MR image produces an MRS-weighted image shown in Fig.9 (d).

3.3 Exponential companding segmentation

To avoid mosaic effects, we propose a nonlinear regression-like model with spatial resolution registration in (3).

$$ComIm(v,p,g) = \exp\left[\frac{MRIm(p,g)}{T} \times MetaR(i,v)\right] + MetaR(j.v) \tag{3}$$

where "T" is a time constant corresponding to *MRIm* (p,g).
According to the correlation model of Table 4, the Lip/Cr and Lac/Cr are specific features w dependent on the tumor grade. So, in the model of equation (2), we have:

$$i \in \mathbf{I}, j \in \mathbf{J}, \quad MetaR = \mathbf{I} \bigcup \mathbf{J}$$
$$\mathbf{I} = \{Cho/Naa, Cho/Cr, mI/Cr\}$$
$$\mathbf{J} = \{Lip/Cr, Lac/Cr\}$$

Because the **J** of *MetaR* is the grade marker, it takes an interceptive role to make a different grey level from other voxels and indicates a variable grade.

3.3.1 Example of exponential companding segmentation

The segmentation method consists of 5 steps:

Step 1. Processing CSI data to get the relative quantitation of MRS, a ratio of peak amplitude or area between 2 metabolites, such as Cho/Naa, as shown in Fig. 9 (c).

Step 2. Extracting brain from original T2-weighted image, and selecting image slices contained in the volume of CSI as shown in Fig.10 (I).

Step 3. Combining the MRS ratio and the grey level information of selected image slices by multiplying the ratio of MRS, e.g. Cho/NAA, to attain MRS-weighted images as mentioned in 3.2, and shown in Fig.10 (II).

Step 4. Exponential companding to extend the difference of grey levels between normal tissue and tumor, is done as (2), and shown in Fig.10 (III).

$$ExpIm(v,p,g) = \exp(ComIm(v,p,g)/T) \tag{2}$$

where "T" is a time constant corresponding to *ComIm* and it is determined by the first peak of *ComIm*'s histogram.

Step 5: Tumor area segmentation by region growing, with the brightest pixel selected automatically as seed. The results are shown in Fig.10 (IV).

3.3.2 Material

The test data consists of CSI raw data and T2-weighted image. These data were acquired with STEAM sequence at the Beijing Tiantan hospital (China), with Siemens MR TrioTim (3T) and syngo MR B15. The MRS raw data are measured by csi_st/90 protocol with TR3000/TE72/TM6. T2-weighted images are measured by t2_tse_tra protocol with TR4500/TE80. An example of original test data is shown in the first row of Fig. 7.

The resolution of T2 is 0.57×0.57mm^2 pixel size and 5mm slice thickness. It can be noted as an image voxel of 0.57×0.57×5 mm^3. The CSI location image shows that the MRS voxel size is 14×14×20mm^3. According to the header information of CSI raw data, we can locate 3 ordinal slices of T2, as shown in Fig. 10(I).

3.3.3 Segmentation results

The first step is to process the CSI data to obtain the metabolite ratio. We use THU-MRS1.0, a software tool developed by our research group (Dou et al., 2009; Chi et al., 2011) for automated processing and quantitative analysis of MRS data, to calculate Cho/Naa voxel-by-voxel. An example is shown in Fig.9.

The segmentation result is shown in the fourth row of Fig.10. The output of each step of our method can be observed in Fig.10. The first row shows the result from step 2: 3 slices of original T2 contained in the volume of CSI. The second row shows the results of step 3: the product of the T2 intensity value and the ratio of MRS. The output of step 4, the exponential companding result, is shown in the third row.

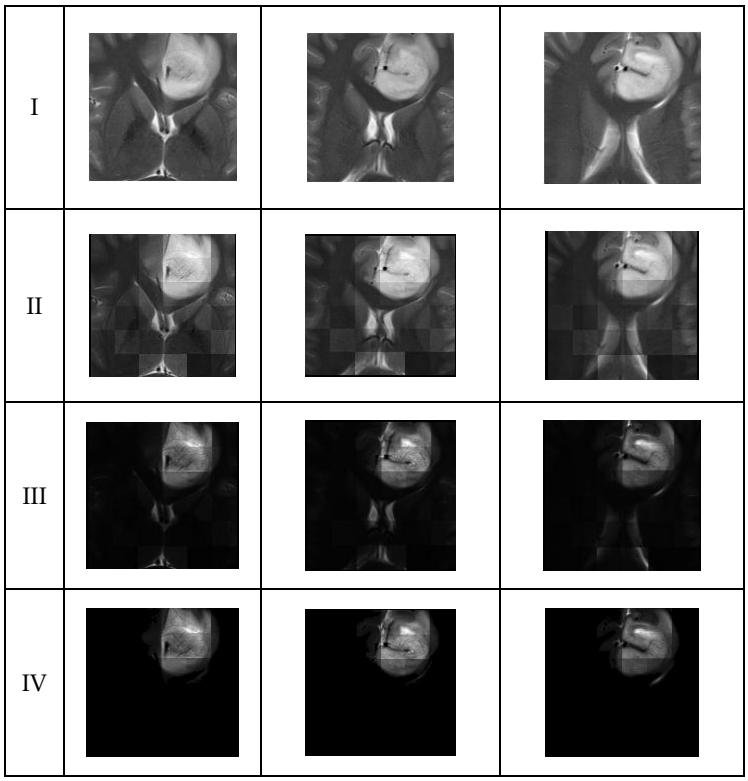

Fig. 10. Experiment results inside VOI of CSI. The first row shows 3 slices of original T2, which are contained in the volume of CSI, and resulting from step 2 of the proposed method; the second row presents the results of step 3, the third row resulted from step 4; and the last row represents the segmentation result from step 5.

3.3.4 Result evaluation

To evaluate the efficiency of our proposed method, we define the ratio of correct detection P_c and false detection P_f as (3) and (4), respectively.

$$p_c = \frac{N_{TruePositive}}{N_{RTumor}} \times 100\% \tag{3}$$

and

$$p_f = \frac{N_{FalsePositive}}{N_{RNormal}} \times 100\% \tag{4}$$

where $N_{RNormal}$ is the number of voxels in the region of normal brain tissues, and N_{RTumor} is that in the region of tumor tissues, as shown inside the red line in Fig.11. So, the total voxel number inside the VOI (white square in Fig.11) is the sum of $N_{RNormal}$ and N_{RTumor}. $N_{TruePositive}$ is the number of voxels which are detected as true positives and $N_{FalsePositive}$ is that of false positives.

A true or false positive is related to a standard model, called "ground truth". In our experiment, the ground truth is determined by manual labeling by 2 neuroradiologists, shown as a red circle in Fig.11. the first row is the "ground truth" of tumor plus potential edema area, called G1, and the second row is that of tumor only, called G2.

Comparing the segmentation result and the "ground truth", we obtain the evaluation results presented in Table 5. The correct detection rate is 98.89% for tumors with edema, and 99% for tumor only. The false detection rate in VOI is 6.48% for tumor with edema and 9.34% for tumor only.

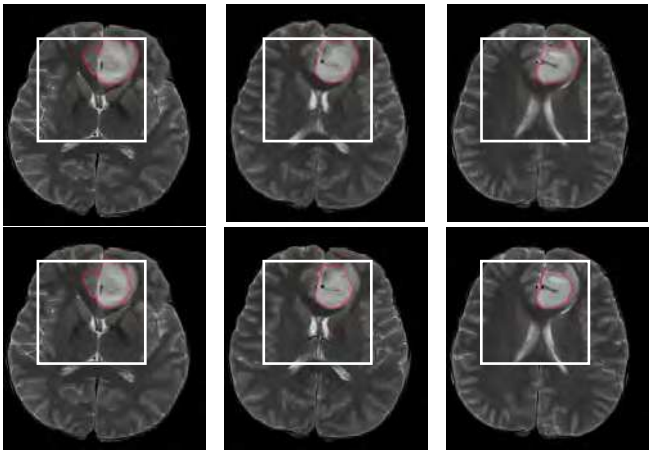

Fig. 11. The manual label results with potential edema, G1 (the first row), and without edema or tumor only, G2 (the second row).

4. Discussion

MRI remained stable for all patients, except for 2 late partial responses. MRS showed variable ratios of mI/Cr, Cho/Cr and NAA/Cr at baseline. We observed a decrease in Cho/Cr ratio and mI/Cr (to a lesser extent) and an increase in NAA/Cr ratio for patients whose clinical conditions improved and the reverse results for those whose conditions deteriorated.

Chemotherapy, radiation, and antiangiogenic therapies are widely used in the treatment of malignant brain tumors (Stupp et al., 2009; Tuettenberg et al., 2006), especially in gliomatosis that is inoperable, often leading to a mass effect in the progression, motor or language deficits or seizures and and development into high grade gliomas. Temozolomide was well tolerated. Patients had initial clinical and MRS improvement and stable MRIs. After 18 cycles, MRS showed an increase in the Cho/Cr ratio (proliferation). However, later in progression in 4 patients with hyperperfusion, this disappeared but proliferation (Cho/Cr), infiltration (NAA), and glycolytic metabolism (lactate) remained at a high level.

The glial tumor segmentation method using data fusion and exponential companding, is sensitive to the results of CSI processing and the quantitative analysis of MRS. The area ratio of metabolites is widely used in clinics when using single voxel spectroscopy (SVS). However, when using CSI data, the partial volume effects will affect neighboring voxels. It is then difficult to get a perfect MRS. In our experiment, the amplitude ratio of metabolites is better than area ratio because it is not as sensitive to processing results as the area ratio.

We used only one metabolite ratio, Cho/Naa, in our experiment, but for tumor grade definition the Lac and Lip are useful. An improved study will focus on CSI processing, data combination among other metabolites and other MR images, eg, T1-weighted, FLAIR, and gadolinium.

Ground truth	**Segmentation validation in VOI**	
	correct detection **P_c (%)**	***false detection*** **P_f (%) in VOI**
G1	98.89	6.48
G2 (tumor only)	99	9.34

Table 5. Result evaluation of tumor segmentation in VOI

5. Conclusion

The spectroscopic and metabolic changes mentioned here, in addition to improve prognostic assessment (Law et al., 2003), occurred well before clinical deterioration and just before improvement. MRS allows non invasive follow-up of treated cerebral tumors. Therefore, MRS could be more sensitive and could detect changes earlier than MRI and is sometimes predictive.

There is a large amount of variability, but repetition and modelization of spectroscopic measurements during longitudinal follow-up could allow us to diminish it and to improve prognostic evaluation, especially in cases being treated with antiangiogenic therapy.

MRI, spectroscopy (MRS), and perfusion could be useful for monitoring energy (glutamine and glucose), glycolytic metabolism (lactate), necrosis (lipid metabolism), cell proliferation (Cho/Cr), and infiltration (NAA/Cr), and for classifying disease as stable or progressive. **(**Bendszus et al., 2000**).** These changes, as was shown, can be studied longitudinally and non invasively in humans with glial brain tumors after therapies **(**Callot et al., 2008**).** These repeated measures could give us more insight into the evolution at different times of the pathological processes, stages, tumor progression and response to therapies.

It will be important to follow gliomas to see if they become high grade glioma and even glioblastoma (Kannuki et al., 1998) in which we can study anatomical FLAIR, metabolism and proliferation with parameters from other modalities like MR, PET (11C-MET and 18F-FLT (Valable et al., 2011) and MRS. Studying the relationship between quantitative MRS measures, PET, MRI segmentation, and perfusion parameters could lead to a better understanding of tumoral pathological processes and therapeutic response, especially with regard to chemotherapy and antiangiogenic molecules, and in the future, hypoxia modulators and antioxidant molecules. These relationships could serve as a priori knowledge or constraints to improve fusion between CSI and MRI.

The segmentation method using data fusion of MRI and MRS is only a simple information fusion strategy, but it is effective for image segmentation. There are 2 important steps in this method: data combination and exponential companding; here, they act as image enhancement. It is a good example of image segmentation using data fusion of multimodal signals.

6. Acknowledgment

We would like to extend our thanks to Shaowu Li, professor of the Neuroimaging Center of Tiantan Hospital, Capital Medical University, Beijing, China, for his hard work on data scanning and his diagnostic experience; thanks to Yanping Chen, professor of Imaging Diagnostic Center of Nanfang Hospital, Guangzhou, China, for her hard work on manual labeling; thanks to François Kauffmann, assistant professor in the mathematics department of Caen University, for his hard work on data and signal processing; thanks to our excellent students Solène Collet, Gabriela Hossu, Aoyan Dong, Ping Chi and Shuai Wang for their hard work on some experiments. Also special thanks to Tsinghua National Laboratory for Information Science and Technology (TNList) Cross-discipline Foundation.

7. References

Auer DP, Gössl C, Schirmer T, et al. (2001) Improved analysis of 1H-MR spectra in the presence of mobile lipids. *Magn Reson Med*. 46: 615-8.

Bendszus M, Warmuth-Metz M, Klein R et al. (2000) MR Spectroscopy in Gliomatosis Cerebri, *American Journal of Neuroradiology* 21:375-380

Brandao, L. A. Domingues, R. C., (2003). MR spectroscopy of the brain, *Livraria e Editora Revinter Ltda*. 2003

Callot V, Galanaud D, Le Fur Y, et al. (2008) 1H MR spectroscopy of human brain tumours: a practical approach, *European Journal of Radiology* 67(2):268-274

Chi, P. Dou, W. Constans, J-M.,(2011). A Post-processing Approach of HLSVD Used for Automatic Quantitative Analysis of Multi-voxel Magnetic Resonance Spectra, *Proceedings of The 5th international conference on bioinformatics and biomedical engineering (iCBBE2011)*, May 10-12, 2011, Wuhan, China.

Chechin D, (2001) Méthode de traitement et de filtrage de signaux de SRM cérébrale proton simple volume, PhD Thesis.

Constans J.M., (2006) Sources de variabilité en SRM proton simple volume quantitative court TE STEAM chez des volontaires sains, PhD.thesis, 2006.

Delcroix N., (2000) Construction d'un système à base de connaissances pour le traitement du signal en spectroscopie 1H simple volume, PhD Thesis, Caen University, France.

Dou, W. Ren, Y. Chen, Y. Ruan, S. Bloyet, D. and Constans, J-M., (2005a). Histogram-based Generation Method of Membership Function for Extracting Features of Brain Tissues on MRI Images, *LNAI,* Vol.3613, 2005, pp.189-194.

Dou, W. Wu, Q. Chen, Y. Ruan, S. & Constans, J.-M., (2005b). Fuzzy modelling of different tumorous cerebral tissues on MRI images based on fusion of feature information, *Proceedings of 27th Annual International Conference of the IEEE Engineering in Medicine and Biology Society (EMBC 2005),* pp.1-4, Shanghai, China, September 2005.

Dou W., (2006) Segmentation d'images multispectrales basées sur la fusion d'informations:application aux images IRM, PhD. thesis, 2006, Caen University, France.

Dou, W. Ruan, S. Chen, Y. Bloyet, D. & Constans, J.-M. (2007a). A framework of fuzzy information fusion for the segmentation of brain tumor tissues on MR images, *Image and Vision Computing,* Vol.25, 2007, pp. 164–171.

Dou W, Ren Y, Constans JM et al. (2007b) Fuzzy Kappa Used for the Agreement measure of Fuzzy Classifications. *Neurocomputing* Vol.70, 2007, pp:726-734.

Dou, W. Wang, S. Li, S. Constans, J-M.,(2009). Automatic Data Processing to Relative Quantitative Analysis of 1H MR Spectroscopy of Brain, *Proceedings of The 3rd international conference on bioinformatics and biomedical engineering (iCBBE2009)*, June 11-16, 2009, Beijing, China.

Dou, W. Dong, A. Chi, P. Li, S. Constans, J-M.,(2010). Glioma Tissue Modeling by Combining the Information of MRI and in vivo Multivoxel MRS, *Proceedings of The 4th international conference on bioinformatics and biomedical engineering (iCBBE2010)*, June 18-20, 2010, Chengdu, China.

Dou, W. Dong, A. Chi, P. Li, S. Constans, J-M.,(2011). Brain Tumor Segmentation Through Data Fusion of T2-Weighted Image and MR Spectroscopy, *Proceedings of The 5th*

international conference on bioinformatics and biomedical engineering (iCBBE2011), May 10-12, 2011, Wuhan, China.

Galanaud D, Nicoli F, Confort-Gouny S, et al. (2007) Indications for cerebral MR proton spectroscopy in 2007. *Rev Neurol*.; 163(3):287-303

Galanaud D, Chinot O, Nicoli F, et al. (2003) Use of proton magnetic resonance spectroscopy of the brain to differentiate gliomatosis cerebri from low-grade glioma. *J Neurosurg*. 98: 269-76.

Garcia-Gomez, J. Luts, J. Julia-Sape, M. Krooshof, P. Tortajada, S. Vicente, J. Melssen, W. Fuster-Garcia, E. Olier, I. Postma, G. Monleon, D. Moreno-Torres, A. Pujol, J. Candiota, A.-P. Martinez-Bisbal, MC. Suykens, JAK. Buydens, L. Celda, B. Van Huffel, S. Arus, C. & Robles, M. (2009) Multiproject-multicenter evaluation of automatic brain tumor classification by magnetic resonance spectroscopy, *Magnetic Resonance Materials in Physics, Biology and Medicine,* vol. 22, (Feb. 2009), pp. 5-18.

Gill SS, Thomas DG, Van Bruggen N, et al. (1990) Proton MR Spectroscopy of intracranial tumors: in vivo and in vitro studies. *J Comput Assist Tomogr*. 14: 497-504.

Guo Y., Ruan S., Landré J., Constans J-M., (2010) A Sparse Representation Method for Magnetic Resonance Spectroscopy Quantification. *IEEE Trans Biomed Eng*. 57(7):1620-7.

Hart MG, Grant R, Garside R, Rogers G, Somerville M, Stein K, (2008) Temozolomide for high grade glioma, Cochrane Database Syst Rev. **2008** Oct 8;(4):CD007415

Hoa, D. (September 2009). Metabolites Explored in 1H-MRS, September 2009, Available from http://www.imaios.com/en/e-Courses/e-MRI/Magnetic-Resonance-Spectroscopy-MRS

Hossu G, (2009) Spectroscopie quantitative par Résonance Magnétique proton en conditions cliniques: étude de la variabilité d'un dispositif ERETIC et spectres de médicaments, PhD Thesis, France, 2009

Howe FA. Opstad KS. (2003a). 1H MR Spectroscopy of brain tumors and masses. *NMR Biomed*. 16: 123-31.

Howe, FA. Barton, SJ. Cudlip, SA. Stubbs, M. Saunders, DE. Murphy, M. Wilkins, P. Opstad, KS. Doyle, VL. McLean, MA. Bell, BA. & Griffiths JR. (2003b). Metabolic profiles of human brain tumors using quantitative in vivo 1H magnetic resonance spectroscopy. *Magn Reson Med*. Vol.49, No.2, (Feb. 2003), pp.223-32.

Kannuki S, Hirose T, Horiguchi H, et al. (1998) Gliomatosis cerebri with secondary glioblastoma formation: report of two cases, *Brain Tumor Pathol*. 15(2):111-6

Kuesel AC, Sutherland GR, Halliday W, et al. (1994) 1H MRS of high grade astrocytomas: mobile lipid accumulation in necrotic tissue. *NMR Biomed*. 7: 149-155

Law M, Yang S, Wang H et al. (2003) Glioma grading: sensitivity, specificity, and predictive values of perfusion MR imaging and proton MR spectroscopic imaging compared with conventional MR imaging. AJNR Am J Neuroradiol. 2003;24(10):1989-98

Luts, J. Laudadio, T. Martinez-Bisbal, MC., Van Cauter, S. Molla, E. Piquer, J. Suykens, JAK. Himmelreich, U. Celda, B. & Van Huffel, S. (2009). Differentiation between brain metastases and glioblastoma multiforme based on MRI, MRS and MRSI'', *in Proc. of the 22nd IEEE International Symposium on Computer-Based Medical Systems (CBMS),* pp. 1-8, Albuquerque, New Mexico, Aug. 2009.

Majós, C. Aguilera, C. Cos, M. Camins, A. Candiota, AP. Delgado-Goñi, T. Samitier, A. Castañer, S. Sánchez, JJ. Mato, D. Acebes, JJ. & Arús, C. (2009). In vivo proton magnetic resonance spectroscopy of intraventricular tumours of the brain, *Eur Radiol.* Vol.19, No.8, (Aug. 2009), pp.2049-59.

Maudsley, AA. Domenig, C. Govind, V. Darkazanli, A. Studholme, C. Arheart, K. & Bloomer, C. (2009). Mapping of brain metabolite distributions by volumetric proton MR spectroscopic imaging (MRSI), *Magnetic Resonnance in Medicin,* Vol.61, (2009), pp.548-559.

Naressi A. (2001) Parametric quantive method and simulation with cerebral metabolites knowledge from modelisations of spectroscopic signatures (jMRUI) and physical properties of molecules. *Computers in Biol. and Med* 31: 269.

Nelson SJ, Graves E, Pirzkall A, et al. (2002) In vivo molecular imaging for planning radiotherapy of gliomas: an application of 1H MRSI. *J Magn Reson Imaging*. 16: 464-476

Nelson S., (1989) Semi-parametric method. *J. Magn. Reson. Imag*. 84: 95.

Preul, MC. Caramanos, Z. Collins, DL. Villemure, J-G. Leblanc, R. Olivier, A. Pokrupa, R. & Arnold, D. (1996) Accurate, non-invasive diagnosis of human brain tumors by using proton magnetic resonance spectroscopy. *Nat Med,* Vol.2, (1996), pp.323–325.

Provencher S., (1982) Parametric method (LCModel) with cerebral metabolites knowledge from modelisations of spectroscopic signatures. *Comput. Phys. Commun* 27: 213.

Soffietti R, Baumert BG, Bello L, Von Deimling A, Duffau H, Frénay M, Grisold W, Grant R, Graus F, Hoang-Xuan K, Klein M, Melin B, Rees J, Siegal T, Smits A, Stupp R, Wick W, (2010) Guidelines on management of low-grade gliomas: report of an EFNS–EANO† Task Force, European Journal of Neurology, Vol17, Issue 9,p 1124-1133, September 2010

Stubbs M, Veech RL, Griffiths JR, (1995) Tumor metabolism: the lessons of magnetic resonance spectroscopy. *Adv Enzyme Regul*. 35: 101-115.

Stupp R, Hegi M, Mason W, et al., (2009) Effects of radiotherapy with concomitant and adjuvant temozolomide versus radiotherapy alone on survival in glioblastoma in a randomised phase III study: 5-year analysis of the EORTC-NCIC trial, *The Lancet Oncology* 10: 459 - 466,

Tuettenberg J, Friedel C, Vaikoczy P, (2006) Angiogenesis in malignant glioma - A target for antitumor therapy? *Crit Rev Oncol Hematol* 59:181-193

Valable S, Petit E, Roussel S et al Complementary information from MRI and [18F]-FMISO PET in the assessment of the response to an anti-angiogenic treatment in a rat brain tumor model, Nuclear Medicine and Biology, in press

Wang, Q. Eirini Karamani Liacouras, Erickson Miranda, Uday S. Kanamalla, and Vasileios Megalooikonomou, (2007). Classification of brain tumors using MRI and MRS data, *Proc. SPIE* 6514, (2007) pp.65140S-1~8.

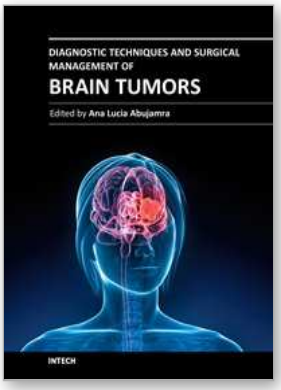

Diagnostic Techniques and Surgical Management of Brain Tumors
Edited by Dr. Ana Lucia Abujamra

ISBN 978-953-307-589-1
Hard cover, 544 pages
Publisher InTech
Published online 22, September, 2011
Published in print edition September, 2011

The focus of the book Diagnostic Techniques and Surgical Management of Brain Tumors is on describing the established and newly-arising techniques to diagnose central nervous system tumors, with a special focus on neuroimaging, followed by a discussion on the neurosurgical guidelines and techniques to manage and treat this disease. Each chapter in the Diagnostic Techniques and Surgical Management of Brain Tumors is authored by international experts with extensive experience in the areas covered.

INTECH
open science | open minds

InTech Europe
University Campus STeP Ri
Slavka Krautzeka 83/A
51000 Rijeka, Croatia
Phone: +385 (51) 770 447
Fax: +385 (51) 686 166
www.intechopen.com

InTech China
Unit 405, Office Block, Hotel Equatorial Shanghai
No.65, Yan An Road (West), Shanghai, 200040, China
中国上海市延安西路65号上海国际贵都大饭店办公楼405单元
Phone: +86-21-62489820
Fax: +86-21-62489821